

PREDICTION OF THE TURBULENT BOUNDARY LAYER DEVELOPMENT BY THE LAG-ENTRAINMENT METHOD

TAHIR YAVUZ

Department of Mechanical Engineering, Karadeniz Technical University, 61080 Trabzon, Turkey

AND

SERPİL ÖZKILIÇ

Erciyes University, Kayseri, Turkey

SUMMARY

The lag-entrainment method, which is a well-established integral method for predicting the development of turbulent boundary layers, is used in this study to predict two-dimensional turbulent separated flow. The method is used in an inverse mode, in which the displacement thickness is specified together with other integral parameters of the boundary layer. It is concluded that the prediction of two-dimensional separated flow by an integral method is feasible, but there is a need for accurate data for both equilibrium and general separated flows for making a comparison.

KEY WORDS Turbulent Lag-entrainment Boundary layer Separation

INTRODUCTION

Turbulent boundary layers in a pressure gradient is a topic of great interest, as they exist, for instance, on aerofoils, fluid machinery blades, diffusers and rocket nozzles. The performance of various kinds of fluid machinery and apparatus is limited by flow separation in the passages, and aerodynamic performance characteristics of the wing depend on the flow separation phenomenon occurring on it. Therefore, it is of vital importance in fluid engineering to establish a procedure to predict if and where the separation flow takes place.

Turbulent boundary layers are 'thin' and possess a predominant flow direction, characterized by the absence of downstream to upstream influence either through diffusive processes or pressure effects. The nature of such a flow on a flat plate is essentially a complicated one, the flow being dominated on one boundary by the pressure of the wall, while at the free-stream edge it is significantly affected by the upstream history of the flow.

The objective of a boundary layer method is the prediction of the mean properties of the flow. Various amount of output are given by the different methods. The boundary layer approach, using continuity, momentum and energy equations, is most widely used by investigators to solve the classical flow separation problems. Through the boundary layer approach, steady, two-dimensional external separation, such as the flow separation over an aerofoil was successfully solved for laminar as well as turbulent flow.

The flow of the separation region is characterized by the interaction between a viscous or dissipative flow near the surface of a solid body and on an 'outer', nearly isentropic stream.

Commonly used separation criteria for steady, incompressible and two-dimensional boundary layers are divided into three groups. The first is based on the skin-friction coefficient, which is zero at the separation point.¹ The second group is based mainly on the pressure distribution of the free stream,^{2,3} and the last group is based on shape parameters which characterize the velocity profile in the boundary layer. Although there are various methods to define and evaluate shape parameters,^{4,5} the shape factor $H = \delta^*/\theta$ of von Doenhoff–Jedervin’s method⁶ is simple and the most widely used. Sandborn⁷ proposed a separation criterion based on two parameters. These are the shape parameter, H , and the pressure gradient parameter, $(\theta^2/\nu) (dU_e/dx)$. Any one of these methods correctly predicts the separation point with almost the same degree of accuracy for external flow.⁸ For internal flow, however, these predictions are not satisfactory.⁹ In this paper, the external flow separation has only been considered, and the first criterion was used for determining the flow separation.

The industrial user will usually settle for reasonably accurate predictions of the skin friction, displacement thickness and separation location.

An emphasis on the integral methods rather than the differential methods is based essentially on two considerations:

- (i) That integral methods generally require less computation time than differential methods and, hence, are cost-effective.
- (ii) That differential methods have not yet shown themselves to be substantially superior to integral methods for the types of flows of aeronautical interest.

In the following section, in general, the integral method will be analysed and in later sections this method will be applied for prediction of the turbulent separation of the boundary layer in an adverse pressure gradient.

INTEGRAL RELATIONS FOR TURBULENT BOUNDARY LAYERS

Neglecting the final terms due to the turbulent normal stress in the Navier–Stokes equations, the turbulent boundary layer equations reduce to a convenient form, as follows:

continuity equation

$$\frac{\partial \bar{u}}{\partial x} + \frac{\partial \bar{v}}{\partial y} = 0, \quad (1)$$

momentum equation

$$\bar{u} \frac{\partial \bar{u}}{\partial x} + \bar{v} \frac{\partial \bar{u}}{\partial y} = U_e \frac{\partial U_e}{\partial x} + \frac{1}{\rho} \frac{\partial \bar{\tau}}{\partial y}. \quad (2)$$

It is assumed that the free-stream conditions $U_e(x)$ are known. The boundary layer conditions are:

no-slip

$$\bar{u}(x, 0) = \bar{v}(x, 0) = 0, \quad (3)$$

free-stream matching

$$u(x, \delta_v) = U_e(x).$$

Equations (1) and (2) can be solved for \bar{u} and \bar{v} if a suitable correlation for the total shear stress is known.

As is known, the integral relation for momentum is found by using continuity to eliminate $v(x, y)$ in favour of $u(x, y)$ and then integrating the resulting equation with respect to y across the boundary layer.

The integral of equation (2) across the boundary layer gives the ordinary differential equation,

$$\frac{d\theta}{dx} + (2+H) \frac{\theta}{U_e} \frac{dU_e}{dx} - \frac{\tau_w}{\rho U_e^2} = \frac{1}{\rho U_e^2} \frac{d}{dx} \left(\rho U_e^2 \int_0^\delta \frac{\bar{u}'^2 - \bar{v}'^2}{U_e^2} dy \right), \quad (4)$$

where

$$\theta \text{ (momentum thickness)} = \int_0^\delta \frac{\bar{u}}{U_e} \left(1 - \frac{\bar{u}}{U_e} \right) dy,$$

$$H \text{ (momentum shape factor)} = \frac{\delta^*}{\theta},$$

$$\delta^* \text{ (displacement thickness)} = \int_0^\delta \left(1 - \frac{\bar{u}}{U_e} \right) dy.$$

This equation contains three variables θ , H and C_f . In laminar flow, we could relate H and C_f to θ easily with a one-parameter correlation (see Reference 10), and then solve the von Karman integral relation for $\theta(x)$. In turbulent flow, the interaction between θ , H and C_f is far more complicated and, several if not many, additional relations are needed to achieve a closed system of boundary layer equations.

Thus, for turbulent boundary layer equations, at least, one must select two additional independent relations to provide closure. The possible additional relationships are:

- (i) the law of the wall,
- (ii) the law of the wake,
- (iii) empirical skin-friction correlation formula,
- (iv) mechanical-energy integral relation,
- (v) entrainment-integral relation,
- (vi) turbulent-energy integral relation,
- (vii) higher momentum of momentum equation,
- (viii) polynomial or experimental velocity profile approximation.

Note that the turbulence terms do not contribute explicitly to the integral momentum equation (4). But all integral relations will involve the turbulent stress in some way. The assumptions which permit the evaluation of these terms amount to implicit consideration of the turbulence, and it is at this point that the additional integral equations can implicitly bring in new physics.

In several of the differential and integral methods the closure of the problem is resolved through the introduction of an assumed 'turbulence equation of state', which relates the turbulence quantities to properties of the mean flow field. Such state equations may either be of a 'local' or 'global' nature. More details are given in Reference 1.

The integral methods which incorporate the entrainment concept use two differential types of entrainment function, i.e. 'entrainment equations of state'. The first type relates the entrainment rate E to the properties of the mean flow through an equation of the type²

$$E = KU_t \quad \text{or} \quad E = KU_e,$$

where K is some empirical function of the outer-layer velocity profile shape parameter, and U_r and U_e are the shear velocity and free-stream velocity, respectively. The alternative is to relate the entrainment rate to the turbulence velocity scale, Q , as

$$E = KQ.$$

where K is presumably a universal constant. There are some arguments which suggest that the entrainment rate should scale on the gradient of the turbulence energy in the outer region of the boundary layer, and not upon the energy.

ENTRAINMENT INTEGRAL RELATIONSHIP AND HEAD'S ENTRAINMENT METHOD

A relationship is derived from the assumption that turbulent boundary layers grow by a process of entrainment from the free stream into the boundary layer of non-turbulent flow at the outer edge of the layer. This notion was first proposed by Head² in 1958.

In his analysis, Head assumed that entrainment into the boundary layer should depend on the velocity defect in the outer part of the layer and be independent of viscosity. To specify this, Head defined the entrainment shape parameter,

$$H_1 = \frac{\delta - \delta^*}{\theta}. \quad (5)$$

In the boundary layer, the volume flow rate per unit span, Q , between $y=0.0$ and $y=\delta$ is given by

$$\begin{aligned} Q &= \int_0^\delta \bar{u} dy = U_e \left[\int_0^\delta dy - \int_0^\delta \left(1 - \frac{\bar{u}}{U_e}\right) dy \right] \\ &= U_e(\delta - \delta^*). \end{aligned} \quad (6)$$

The entrainment velocity, V_E , defined as the component of velocity normal to the edge of the boundary layer, is the rate at which the volume rate per unit length changes with x , so that

$$V_E = \frac{dQ}{dx} = \frac{d}{dx} [U_e(\delta - \delta^*)], \quad (7)$$

or, in non-dimensional form

$$C_E = \frac{1}{U_e} \frac{d}{dx} [U_e(\delta - \delta^*)] = f(H_1). \quad (8)$$

In addition, to relate H with H_1 , Head suggested that

$$H_1 = g(H). \quad (9)$$

The functions f and g can be determined from an analysis of the experimental data obtained by both Newman³ and Schubouer and Klebanoff.⁴ The corresponding fitting relationships are

$$f(H_1) = 0.0306(H_1 - 3)^{-0.653}, \quad (10)$$

and

$$g(H) = H_1 = 1.531/(H - 0.7)^{-2.715} + 3.3. \quad (11)$$

These relationships combined with the von Karman integral equation, and the Ludweig and Tillmann skin-friction formula,

$$C_f = 0.246 R_\theta^{-0.268} 10^{-0.678 H}, \quad (12)$$

give what is known as Head's integral analysis of a turbulent boundary layer.

Basic equations of the lag-entrainment method

In compressible flow, the parameters which occur in the lag-entrainment method are defined as:

displacement thickness

$$\delta^* = \int_0^\delta \left(1 - \frac{\rho \bar{u}}{\rho_e U_e}\right) dy,$$

momentum thickness

$$\theta = \int_0^\delta \frac{\rho \bar{u}}{\rho_e U_e} \left(1 - \frac{\bar{u}}{U_e}\right) dy,$$

shape parameters

$$H = \delta^*/\theta = \frac{1}{\theta} \int_0^\delta \frac{\rho}{\rho_e} \left(1 - \frac{\bar{u}}{U_e}\right) dy,$$

$$H_1 = \frac{1}{\theta} \int_0^\delta \frac{\rho \bar{u}}{\rho_e U_e} dy = \frac{\delta - \delta^*}{\theta},$$

skin-friction coefficient

$$C_f = \frac{\tau_w}{(1/2)\rho_e U_e^2},$$

entrainment coefficient

$$C_E = \frac{1}{r \rho_e U_e} \frac{d}{dx} \left(r \int_0^\delta \rho \bar{u} dy \right).$$

In the lag-entrainment method, the boundary layer is defined by three independent parameters: momentum thickness, θ , shape parameter, H , and entrainment coefficient, C_E . The development of these in a given pressure distribution is predicted by the forward integration of three simultaneous ordinary differential equations, neglecting the normal stress term in equation (4) and including the Mach number, M , as compressible effects:

momentum integral equation

$$\frac{d}{dx} (r\theta) = \frac{rC_f}{2} - (H+2-M^2) \frac{r\theta}{U_e} \frac{dU_e}{dx}, \quad (13)$$

entrainment equation

$$\frac{\theta}{dx} \frac{dH}{dH_1} \left\{ C_E - H_1 \left[\frac{C_f}{2} - (H+1) \frac{\theta}{U_e} \frac{dU_e}{dx} \right] \right\}. \quad (14)$$

The rate equation for entrainment is

$$\frac{\theta dC_E}{dx} = F \left| \frac{2.8}{H+H_1} \left[(C_\tau)_{EQ}^{1/2} - \lambda C_\tau^{1/2} \right] + \left(\frac{\theta}{U_e} \frac{dU_e}{dx} \right)_{EQ} - \frac{\theta}{U_e} \frac{dU_e}{dx} \left[1 + 0.075M^2 \frac{(1+0.2M^2)}{(1+0.1M^2)} \right] \right|. \quad (15)$$

In these equations, r is the body radius in axisymmetric flow (or the radius of longitudinal curvature), set to unity in planar flow, and M is the Mach number, considered to be zero for this analysis as an incompressible flow assumption. The various dependent variables and functions in the equations are evaluated from the following relationships⁵:

C_f and local free-stream properties (evaluated from the known surface pressure distribution)

$$R_\theta = \frac{\rho_e U_e \theta}{\mu_e},$$

$$F_C = (1 + 0.2M^2)^{1/2},$$

$$F_R = (1 + 0.056M^2),$$

$$F_C C_{f_0} = \frac{0.01013}{\log(F_R R_\theta) - 1.02} - 0.00075,$$

H and $\frac{dH}{dH_1}$

$$H_1 = 3.15 - \frac{1.72}{H-1} - 0.01(H-1)^2, \quad (16)$$

$$\frac{dH}{dH_1} = - \frac{(H-1)^2}{1.72 + 0.02(H-1)^3}, \quad (17)$$

C_τ and F

$$C_\tau = 0.024C_E + 1.2C_E^2 + 0.32C_{f_0}(1 + 0.1M^2), \quad (18)$$

$$F = \frac{0.02C_E + C_E^2 + 0.8C_{f_0}/3}{0.01 + C_E} \quad (19)$$

equilibrium quantities

$$\left(\frac{\theta}{U_e} \frac{dU_e}{dx} \right)_{EQ_0} = \frac{1.25}{H} \left[\frac{C_f}{2} - \frac{H-1}{0.432H} (1 + 0.04M^2)^{-1} \right], \quad (20)$$

$$(C_E)_{EQ_0} = H_1 \left[\frac{C_f}{2} - (H-1) \left(\frac{\theta}{U_e} \frac{dU_e}{dx} \right)_{EQ_0} \right], \quad (21)$$

$$(C_\tau)_{EQ_0} = [0.024(C_E)_{EQ_0} + 1.2(C_E)_{EQ_0}^2 + 0.32C_{f_0}], \quad (22)$$

$$(C_E)_{EQ_0} = \left(\frac{C}{1.2} + 0.0001 \right)_{1/2} - 0.01, \quad (23)$$

$$\left(\frac{\theta}{U_e} \frac{dU_e}{dx} \right)_{EQ} = \left[\frac{C_f}{2} - (C_E)_{EQ}/H_1 \right] / (H+1). \quad (24)$$

In these equations, C_f is the skin-friction coefficient, C_τ is the shear stress coefficient, C_{f_0} is the skin-friction coefficient in equilibrium flow in zero pressure gradient, EQ and EQ₀ denote the equilibrium conditions in the presence and absence of the secondary influence on turbulent structure, respectively. F_c and F_R are the scaling functions in skin-friction law.

Equations (13)–(24) are arranged in subroutines in the computer program to provide dependent variables, needed to evaluate the basic equations [(13)–(15)] at each stage of the numerical integration.

As will be seen in the following section, several computer runs show that the lag-entrainment method, the so-called direct method, is capable of predicting attached flow. Also, the method can predict a flow in which the Reynolds number increases and so deviates slightly from the equilibrium locus. But, it is not always useful for the prediction of the separated flow. Separation from even a smooth surface tends to be an unsteady process and this, together with the high turbulent levels, has made measurement in the low-velocity region difficult. Therefore, separated flows tend to be more susceptible to three-dimensional effects, which lower the overall accuracy of the data with which prediction values are to be compared. It is, therefore, particularly desirable to compare any prediction method for separated flow with as much experimental data as possible so that an assessment of the accuracy may be made. This method has demonstrated that it is capable of making predictions for both attached and separated flows and good agreement with the experimental data is obtained throughout the region of attached boundary layer flow. But, disagreement occurs when the flow is well-separated and the standard method does not accurately predict the high values of the shape parameter, which has a value of approximately 2.8 at the separation point. The likely error in the prediction of the separated flow is that the value of dH/dH_1 in equation (19) is too low and that the equilibrium locus is inaccurate. The former determines the rate at which the shape parameter tends to its equilibrium value, which itself is determined by the equilibrium locus. It is anticipated that in separated flow the shape parameter will rapidly approach its equilibrium value, which implies a large value of dH/dH_1 in equation (17). As pointed out in Reference 1, it seems sensible when applying the lag-entrainment method to separated flow that increasing dH/dH_1 in equation (17) permits the shape parameter to change rapidly to a quasi-equilibrium, while the entrainment coefficient in equation (15) adjusts more slowly to the new conditions. Therefore, modified relationships are recommended:¹

for $H \leq 1.6$

$$H_1 = 3.15 + 1.72/(H - 1),$$

and

$$dH/dH_1 = -(H - 1)^2/1.72, \quad (25)$$

for $H \geq 1.6$

$$H_1 = 4.5455 + 295 \exp(-3.325H),$$

and

$$dH/dH_1 = -\exp(3.325H)/980. \quad (26)$$

For values of H below 1.6 the standard and modified relationships are essentially the same but differ slightly as the third term on the right-hand side of equation (16) and the corresponding term in equation (25) has been dropped.

THE INVERSE MODE OF THE LAG-ENTRAINMENT METHOD

The standard direct mode of the lag-entrainment method computes the boundary layer development for given starting conditions and a specified externally imposed pressure gradient. In this

section, the inverse mode, in which the pressure distribution is predicted for a given displacement surface, is developed.⁵ For this an explicit equation is required, which expresses the pressure gradient parameter, $(\theta/U_e) \cdot (dU_e/dx)$, as a function of the gradient of the displacement thickness, $d\delta^*/dx$, and other local parameters. $d\delta^*/dx$ can be derived from the definition of H as

$$\frac{d\delta^*}{dx} = \frac{d(\theta H)}{dx} = \theta \frac{dH}{dx} + H \frac{d\theta}{dx}. \quad (27)$$

Using equations (27), (13) and (14), and with some rearrangement, we get

$$\frac{d\delta^*}{dx} = F_1 + F \left(\frac{\theta}{U_e} \right) \left(\frac{dU_e}{dx} \right), \quad (28)$$

where

$$F_1 = \frac{HC_f}{2} + (1 + 0.2rM^2) \left(C_E - \frac{H_1 C_f}{2} \right) \frac{dH}{dH_1},$$

$$F_2 = -H(H + 2 - M^2) + (1 + 0.2rM^2)(H + 1)H_1 \frac{dH}{dH_1} + 0.4rM^2(1 + 0.2M^2)(H + 1).$$

Equation (28) can be written as an explicit equation for $(\theta/U_e)(dU_e/dx)$ in the form

$$\frac{\theta}{U_e} \frac{dU_e}{dx} = \frac{1}{F_2} \left(\frac{d\delta^*}{dx} - F_1 \right). \quad (29)$$

Thus, equation (29), used as a differential equation for U_e , can be integrated together with equations (5)–(7) and is all that needs to be added to the direct mode to provide the inverse mode operation. In this case, the measured displacement thickness was used as the input.

The response of the boundary layer displacement thickness to changes in the imposed pressure gradient is given by equation (28). The first term on the right-hand side represents the growth rate caused by shear stress and contains history effects by way of the entrainment coefficient C_E . The second term represents the growth induced by pressure gradient. More details of the indirect method can be found in Reference 5.

RESULTS AND DISCUSSION

The lag-entrainment method has been applied to the prediction of the two-dimensional turbulent separated flow and operated in an inverse mode, in which the displacement thickness of the layer is specified and the pressure distribution and remaining integral parameters are calculated. When there are substantial regions of both attached and separated flow, a computer programme is used in which the mode changes automatically from the direct (external velocity specified) to the inverse mode whenever the skin friction falls below about 80% of the equivalent flat plate value or H exceeds 1.6.

The direct method has been applied to all flows identified as mandatory test cases of the Stanford Conference.¹¹ The results obtained can be distinguished into two categories:

- (i) The cases of equilibrium boundary layer and relaxing flows: It has been noticed that there is excellent agreement between the results predicted by the direct mode of the lag-entrainment method and the experimental data. Figure 1 shows the comparison between the experiment in which the model was a steam-heated flat plate with a curved leading edge having a small trip wire and the prediction. The free-stream turbulence level in this experiment was about

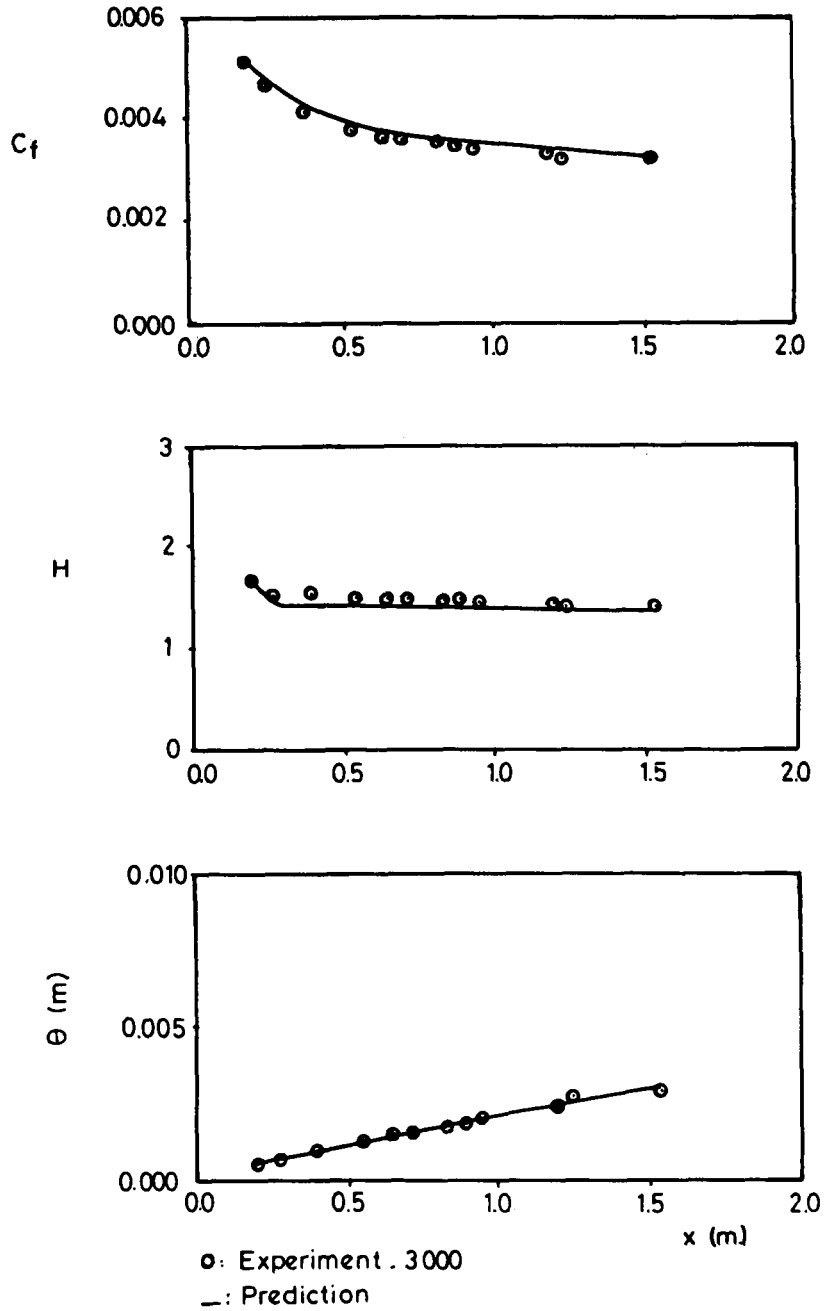


Figure 1. Boundary layer development on the heated plate at a constant pressure (experimental data by Bell, identified as a flow number 3000 at the Stanford Conference¹¹)

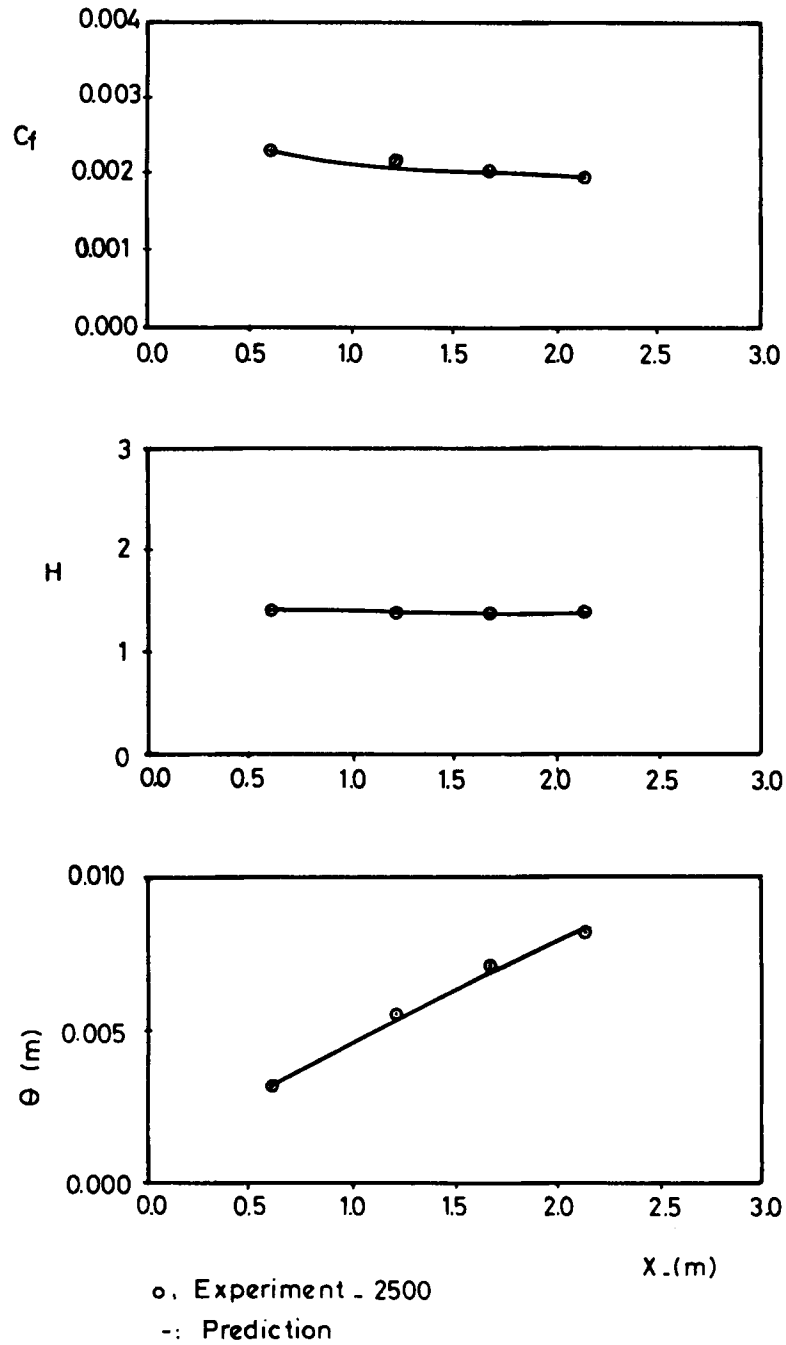


Figure 2. Development of equilibrium boundary layer in a mild positive pressure gradient (experimental data by Bradshaw, identified as a flow number 2500 at the Stanford Conference)

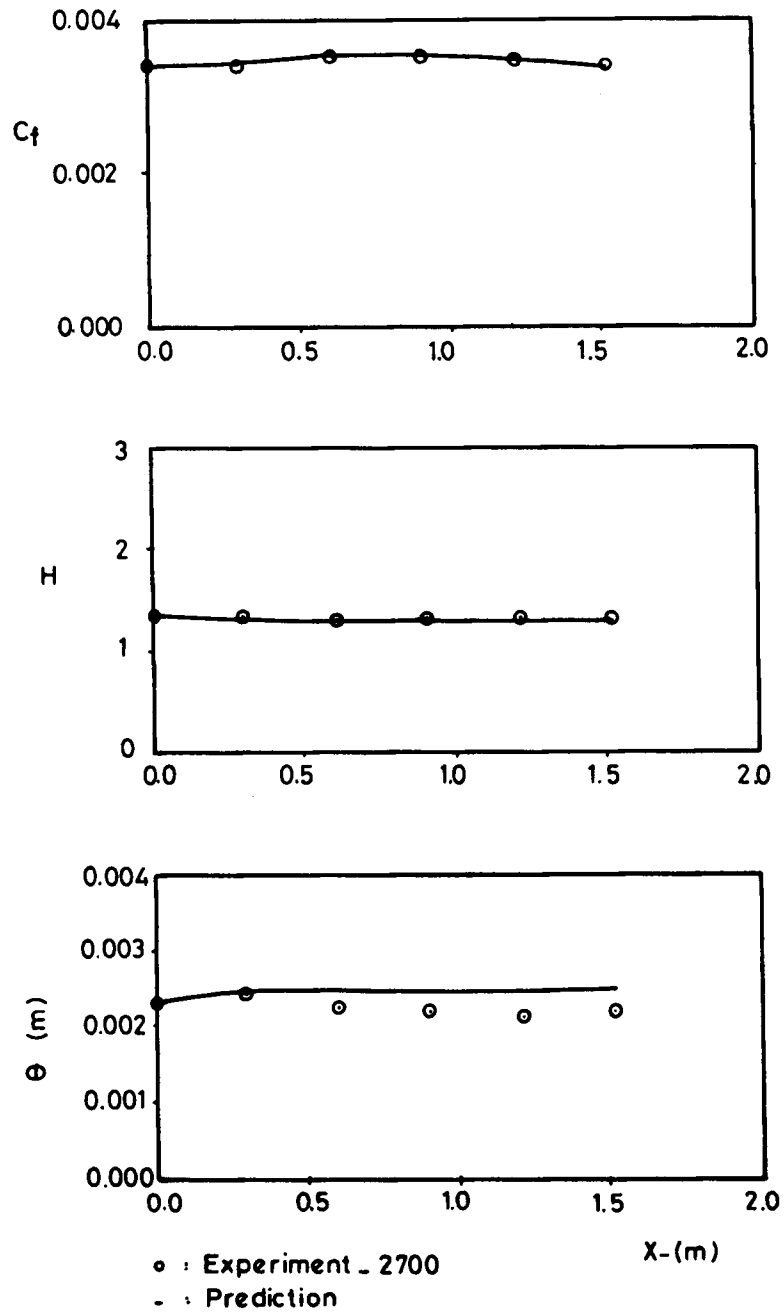


Figure 3. Equilibrium boundary layer in a mild negative pressure gradient (experimental data by Haring and Norbury, flow number 2700¹¹)

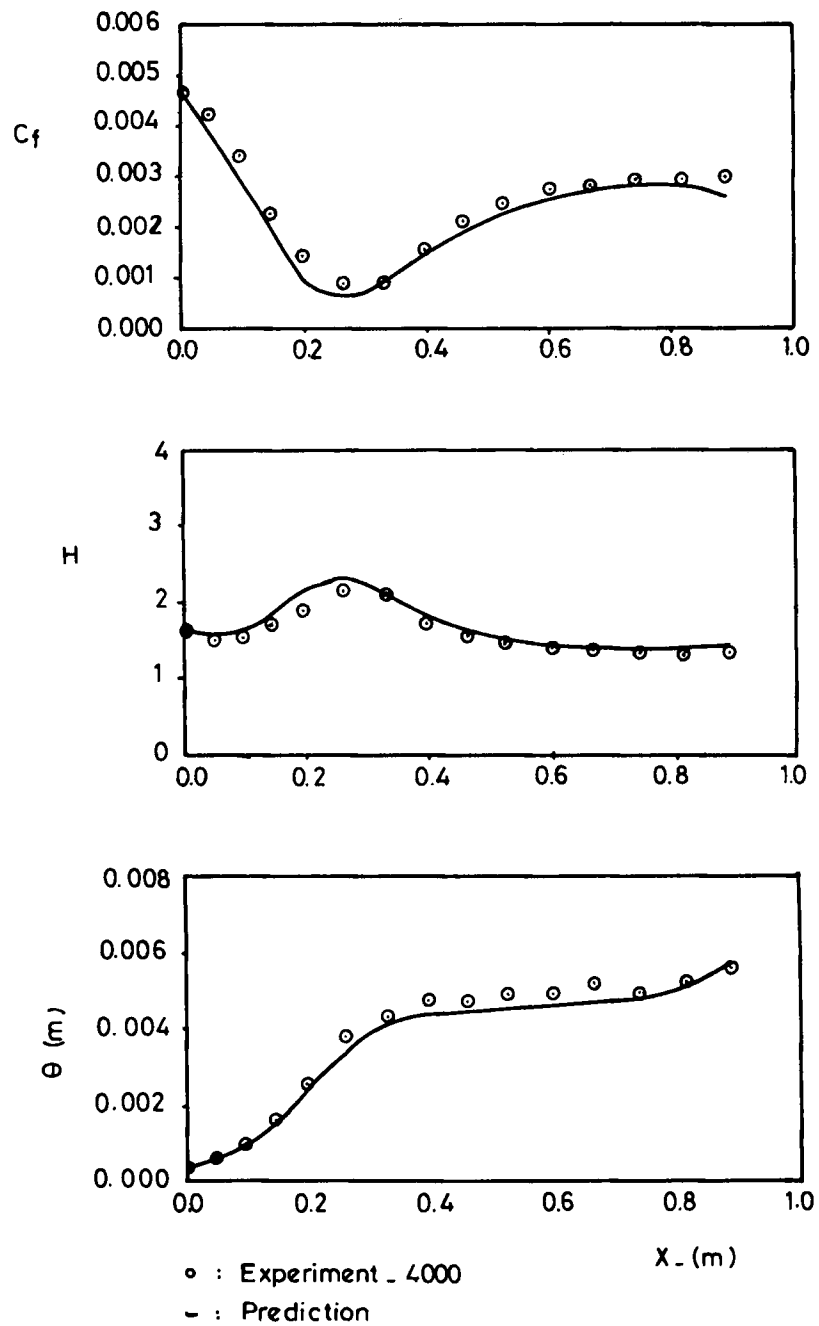


Figure 4. Boundary layer development on a cylinder in an axially symmetric flow with a strong initial pressure rise followed by relaxation at constant pressure (experimental data by Moses, flow number 4000^{14})

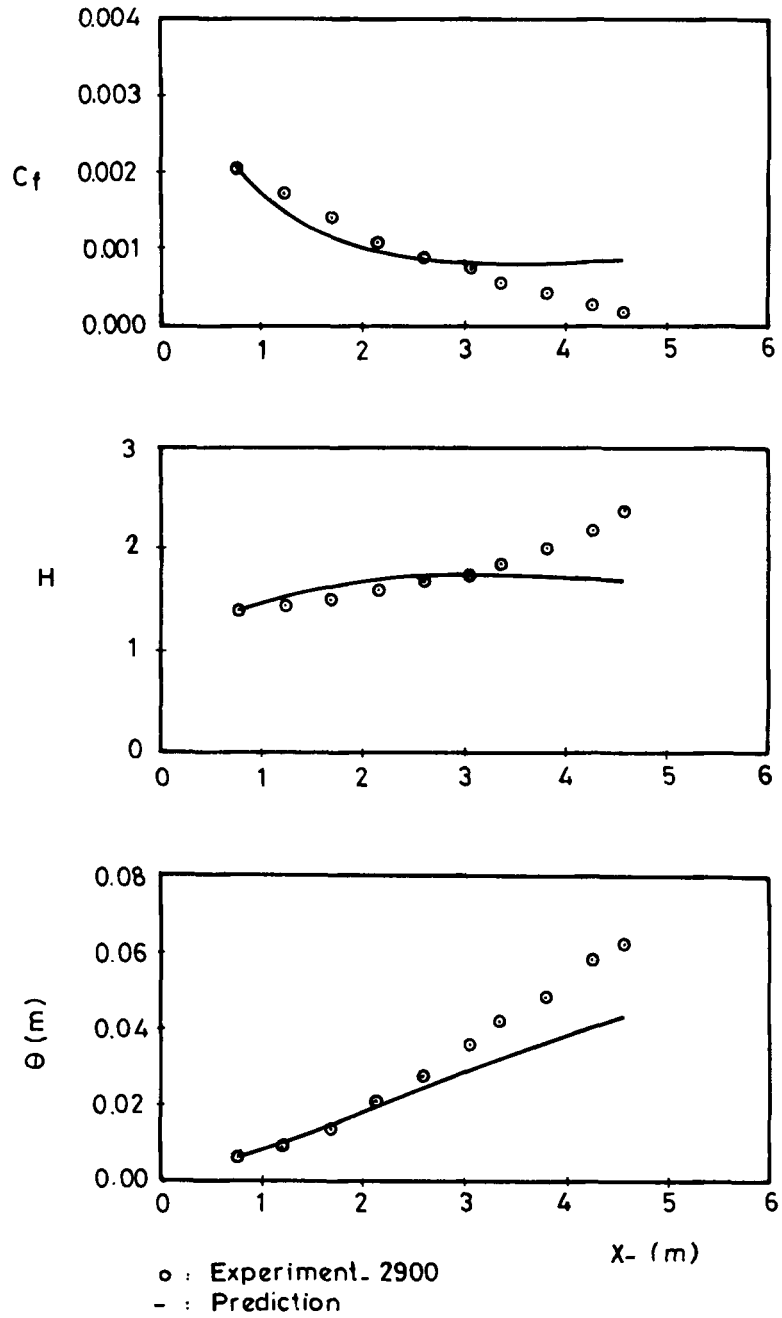


Figure 5. Boundary layer in a diverging channel (decreasing adverse pressure gradient) (experimental data by Perry, flow number 2900¹¹)

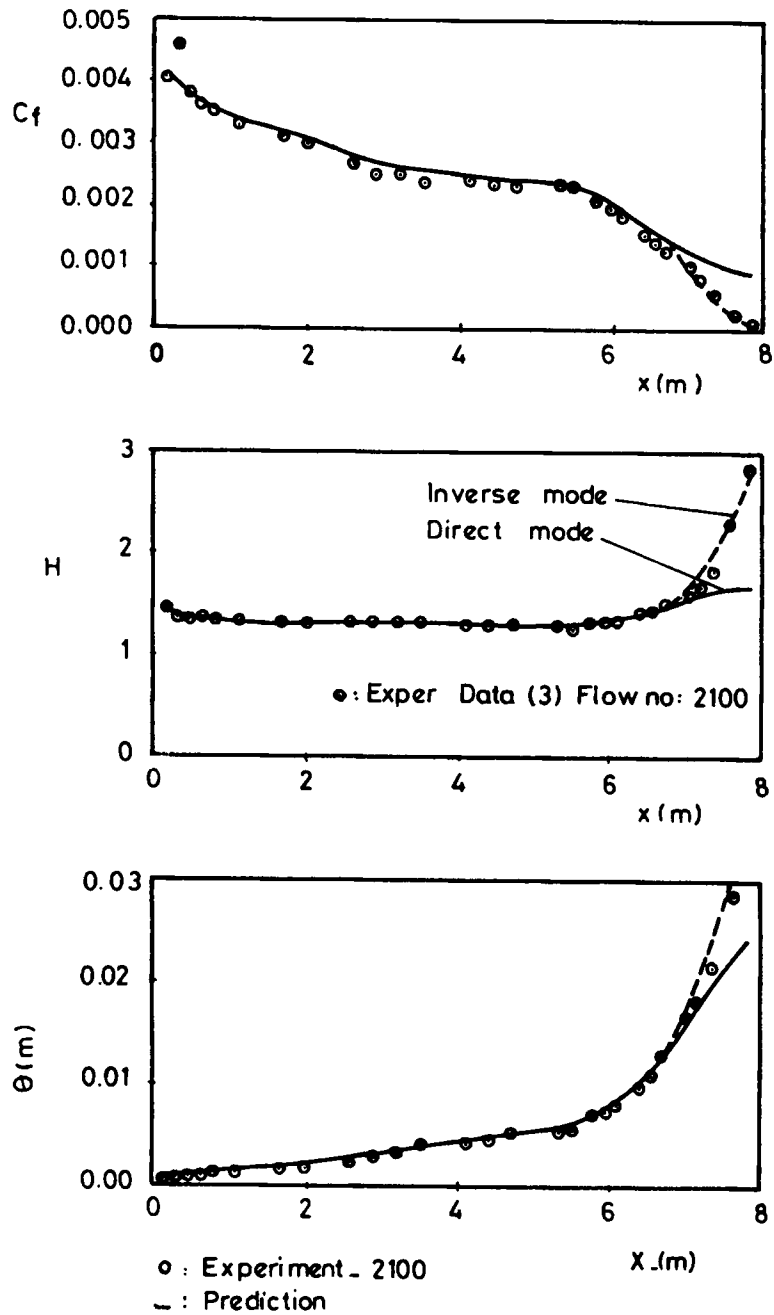


Figure 6. Boundary layer development in a pressure gradient that is first mildly negative and then strongly positive, with eventual separation (experimental data by Schubauer and Klebanoff, flow number 2100¹¹)

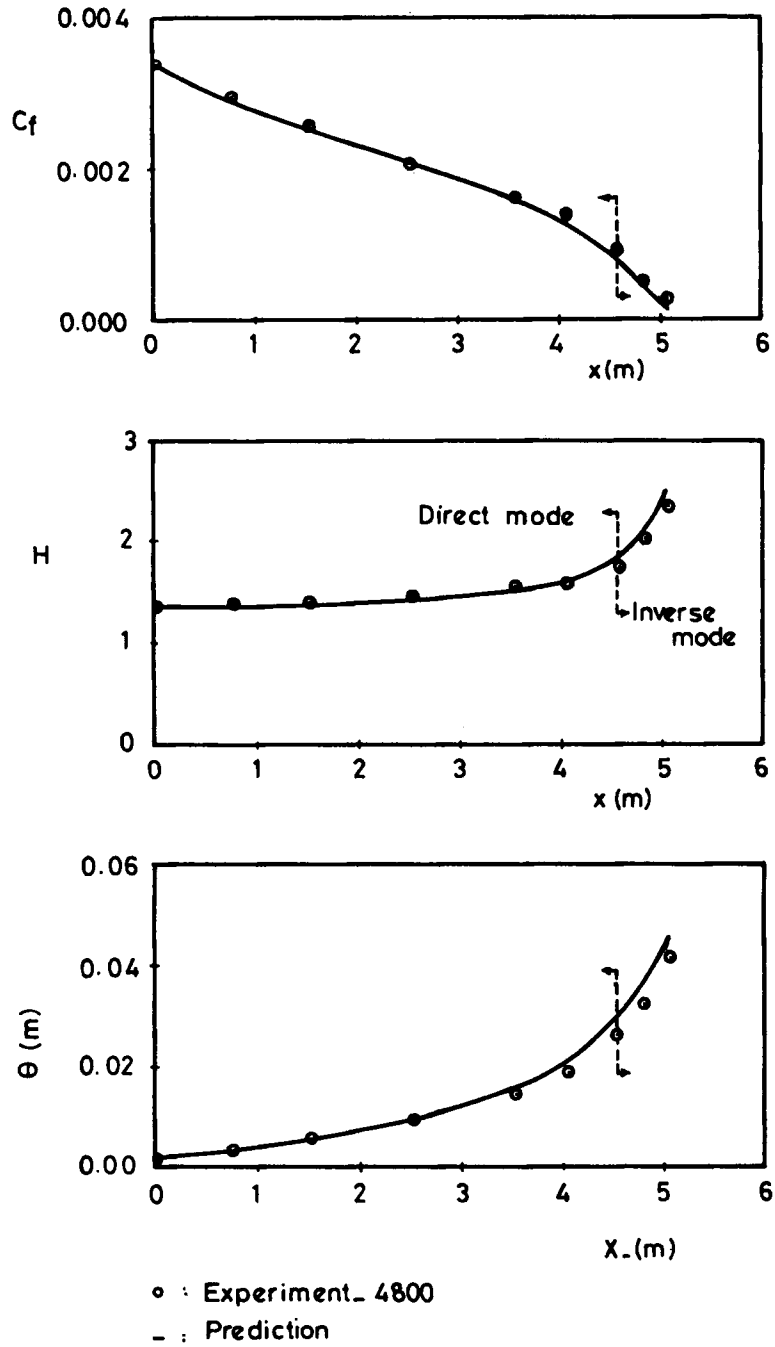


Figure 7. Boundary layer development in a strong adverse pressure gradient (flow number 4800¹¹)

1%. The experimental data in Figure 2 represent the equilibrium boundary layer development determined by Bradshaw in a mild positive pressure gradient. The free-stream turbulence level was less than 0.1%. Figure 3 shows the equilibrium boundary layer development in mild negative pressure gradients. As seen, there is some disagreement between the experimental data and the results predicted for momentum thickness. This might be due to the fact that, according to the editors comment,¹¹ limited information about the pressure distribution makes the pressure gradient somewhat uncertain, but may be relatively high.

Also, Figure 4 shows the comparison between the results predicted and the experimental data obtained by Moses¹¹ on the boundary layer on a cylinder in an axially symmetric flow with a strong initial pressure rise followed by relaxation at a constant pressure.

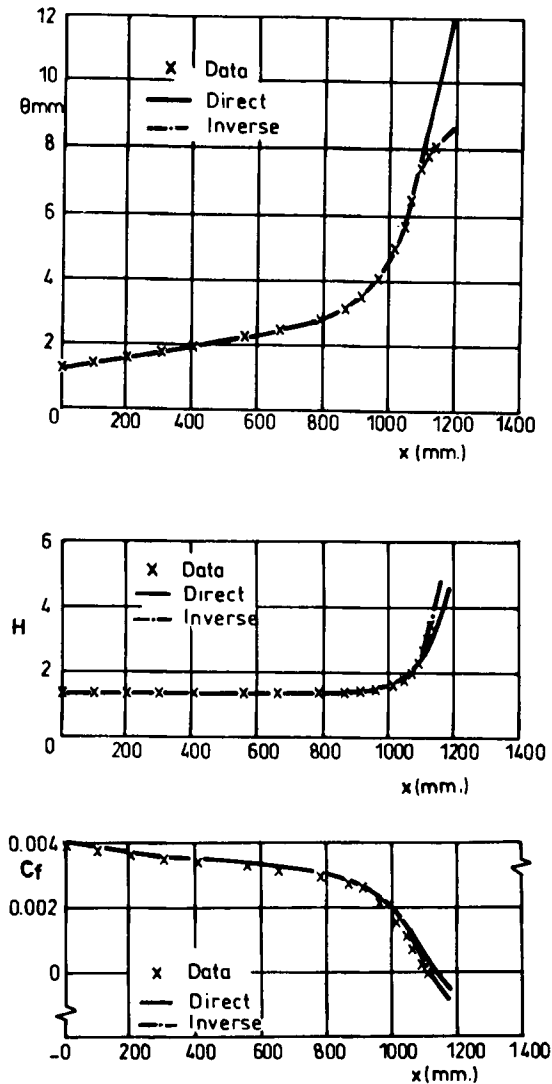


Figure 8. Boundary layer development for a low-speed flow¹²

It has been observed that there is quite a good agreement between the experimental data and the results predicted by the direct mode of the lag-entrainment method for the cases outlined above.

- (ii) Cases of adverse pressure gradient and separation flows: As seen from Figures 5–7, the direct mode has failed to predict higher values of the shape parameter, eventually leading to the separation flow.

The experimental data in Figure 5 represent the boundary layer development in a diverging channel. The disagreement between the predicted and the experimental data becomes higher in the downstream direction. Similar trends can be observed in Figure 6, which represents the boundary layer development on large aerofoil-like bodies for the

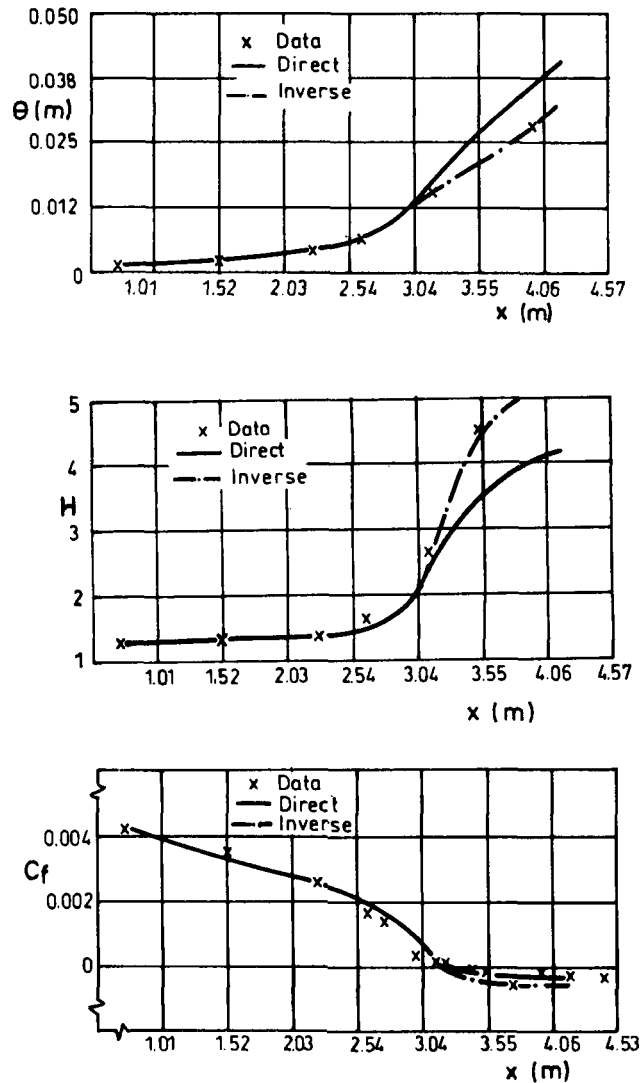


Figure 9. Boundary layer development for a low-speed flow¹³

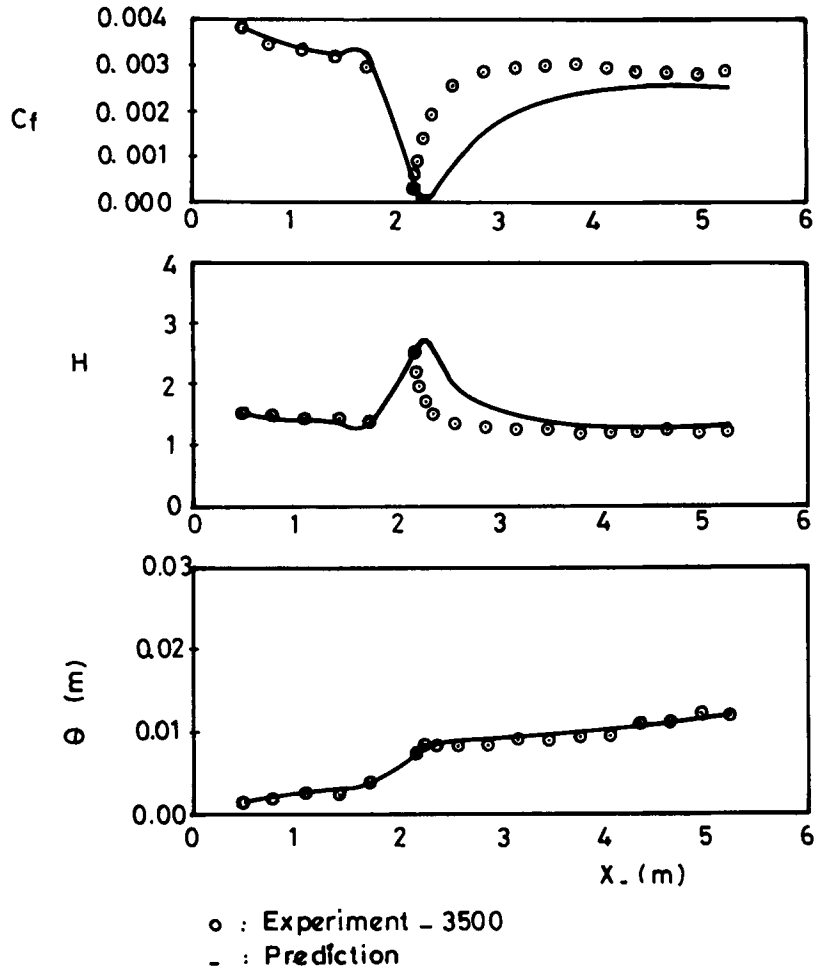


Figure 10. Boundary layer development at nominally constant pressure, with separation and reattachment at a Ledge spoiler (experimental data by Tillmann, flow number 3500¹¹)

pressure gradient first mildly negative and then strongly positive with eventual separation, and in Figure 7, representing the boundary layer development in a strong adverse pressure gradient. In all these cases, the indirect mode has been applied when the shape parameter becomes higher than 1.6. The results predicted by the indirect mode, also shown in these figures with the dashed line, give an acceptable agreement with the experimental data. The results of the direct and indirect modes applied to the low-speed flows of Chu and Young¹² and Simpson¹³ are presented in Figures 8 and 9. Good agreements with the experimental data have been obtained.

Also, the direct mode has been applied to the Tillmann Ledge flow, in which flow occurs at nominally constant pressure, with separation and reattachment at a ledge spoiler. The results are presented in Figure 10. Except in the region near the ledge spoiler, there is good agreement between experiments and prediction.

CONCLUSIONS

The results obtained show that by using an appropriate internal turbulent boundary layer prediction technique, the turbulent flow separation for the external flow can be predicted. The calculations have shown that, whereas the inverse mode can be used to predict both attached and separated flows, only attached flow can be predicted by the direct mode.

The general conclusion drawn from this study is that it is possible to develop an integral calculation method, such as the lag-entrainment method, to predict two-dimensional separated flow to an acceptable accuracy. As can be seen, the normal turbulent term is not considered in the analysis. It could be included and its effect might be important for separated turbulent flow. However, before a prediction method of any kind can be adequately developed, there is a need for more reliable data to be obtained in both equilibrium and non-equilibrium separated turbulent flow in order to make an accurate assessment.

REFERENCES

1. M. R. Head and V. C. Patel, 'An improved entrainment method for calculating turbulent boundary layer development', *A.R.C.R. & M.*, **3643** (1969).
2. M. R. Head, 'Entrainment in the turbulent boundary layer', *A.R.C.R. & M.*, **3152** (1958).
3. A. Naumman, *Z. Angew. Math. Mech.*, **36**, (1956).
4. G. B. Schubauer and R. Klebanoff, *NACA Report 1289*, 1955.
5. L. F. Earl, P. D. Smith and R. J. Merryman, 'Prediction of the development of separated turbulent boundary layers by lag-entrainment method', *RAE Technical Report 77046*, 1977.
6. A. E. Von Doenhoff and N. Tetervin, 'Determination of general relations for the behaviour of turbulent boundary layer', *NACA Report 772*, 1943.
7. V. A. Sandborn and S. J. Kline, 'Flow models in boundary layer stall inception', *J. Basic Eng., Trans. ASME, Series D*, **83**, 317-327 (1961).
8. T. Cebeci, G. J. Mosinskis and A. M. O. Smith, 'Calculation of separation point in incompressible turbulent flows', *J. Aircraft*, **9**(9), 618-624 (1972).
9. P. K. Chang, *Separation Flow*, Pergamon Press, Oxford, 1970.
10. F. M. White, *Viscous Fluid Flow*, McGraw-Hill, New York, 1974.
11. D. E. Coles and E. A. Hurst, 'Vol II, Compiled Data Proceedings. Computation of the turbulent boundary layer', AFOSR-IFP-Stanford Conference, 1968.
12. J. Chu and A. D. Young, 'Measurements in separating two-dimensional turbulent boundary layers', *AGARD CP-168, Paper 13*, 1976.
13. J. Simpson, 'Characteristics of a separated incompressible turbulent boundary layer', *AGARD CP-168, Paper 14*, 1976.